# Busbar technology development for the HL-LHC inner triplet magnets

**E. Tsolakis, L. Favier, R. Principe, H. Prin, F. Meuter, C. Scheuerlein**

European Organization for Nuclear Research (CERN), 1211 Geneva 23, Switzerland

Corresponding author: Christian.Scheuerlein@cern.ch

**Abstract.** The busbars for the HL-LHC magnets are made of Nb-Ti/Cu conductor, the insulation system, and the auxiliary equipment to align the busbars with respect to the magnet coldmasses. This paper presents design options concerning the integration of the busbars inside the coldmass with a fixed point, and a reinforced insulation system for the flexible busbar part using thin PEEK tubes. Prototype splices for interconnecting $Nb_3Sn$ and Nb-Ti Rutherford cables, and round and flat 18 kA Nb-Ti cable have been produced and first test results are presented.

## 1. Introduction

For the high luminosity upgrade of the LHC (HL-LHC) [1], the presently installed quadrupole magnets at the beam interaction regions (IR) (inner triplet magnets) made of Nb-Ti conductor will be replaced by more powerful magnets using $Nb_3Sn$ superconducting cables [2].

The electrical circuits for the HL-LHC triplet magnets contain three distinct sub-circuits of 18 kA, 13 kA and 2 kA. A schematic representation of the 18 kA main, and 18 kA trims circuits are shown in Figure 1. One internal busbar made of flat Rutherford cable is routed through the Q1, Q2 and Q3 cold masses. The more flexible round 18 kA cable with about 14 mm diameter is used for the trims in the N1 line [3]. A flat cable is used for the passage through the lambda plate. The busbar specifications can be found in reference [3].

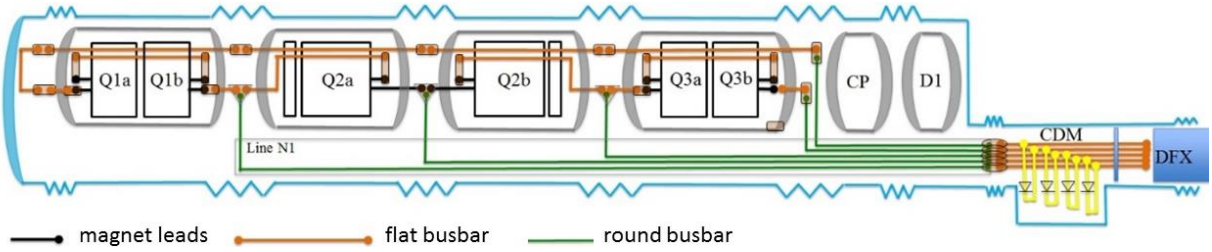


**Figure 1:** Conceptual design of the inner triplet 18 kA circuits [3].

Here we present the ongoing work at CERN for the development of the MQXFB magnet 18 kA busbars, including development of a busbar fixed point, reinforced insulation of flexible busbar parts, and splices.

Content from this work may be used under the terms of the Creative Commons Attribution 3.0 licence. Any further distribution of this work must maintain attribution to the author(s) and the title of the work, journal citation and DOI.
Published under licence by IOP Publishing Ltd

## 2. Busbar design and manufacturing

For the 18 kA busbar circuits three types of conductor will be used, notably 18 kA Nb-Ti flat Rutherford cable for magnet leads and the internal busbars, 18 kA Nb-Ti round cable, used in the N1 line, and 18 kA Cu conductor to connect the cold protection diodes.

### *2.1 18 kA internal busbars*

As compared to the LHC main dipole and quadrupole circuits, the current decay constants of the IR quadrupole circuits are relatively short. Therefore, the cross section of the Cu stabiliser added to the Rutherford cable can be comparatively small. For protection it is sufficient to solder a second identical Nb-Ti cable. The two 18.15 mm wide Nb-Ti Rutherford cables are soldered together and stabilized with the tin-silver eutectic alloy, Sn96Ag4. This alloy has been chosen for its melting point of 221 °C, which is sufficiently low not to degrade the properties of the superconducting cable [4] during the soldering process, and sufficiently high not to be affected by the polymerization heat treatment of the insulation with a peak temperature of 190 °C. The solder material also presents favourable electrical characteristics at low temperature [5]. An internal busbar was successfully manufactured and tested at Fermilab in a MQXF short model. The experimental results have confirmed simulation results that indicate that the busbar is well protected for a quench detection threshold of 100 mV [6]. The measured and calculated hot spot temperatures are compatible with the specified values for HL-LHC as presented in [3].

### *2.2 Internal busbars in the MQXFB coldmass*

Contrary to the design solution adopted for the LHC main dipoles and the 11 T dipole, where the busbar is routed in an external groove at the outer surface of the yokes, in the MQXF quadrupole magnets the busbars are inserted inside the body of the coldmass, as shown in Figure 2.

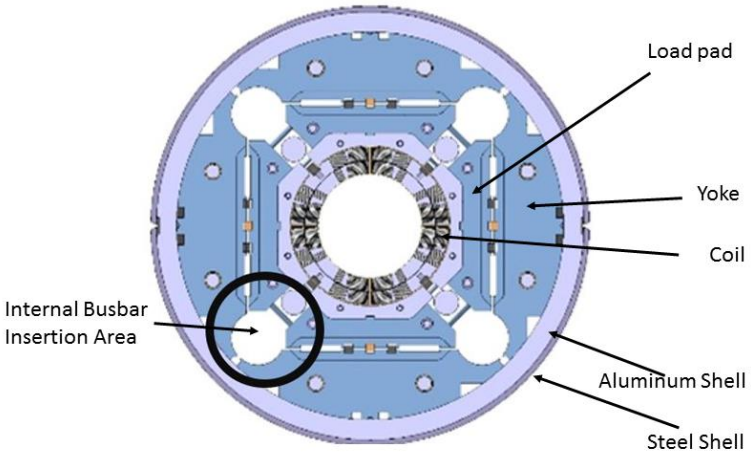


**Figure 2:** Cross section of the MQXFB quadrupole coldmass (∅=614 mm) with main components and indication of the busbar position.

In order to compensate for thermal contraction differences between the busbars and cold masses, busbars need to have a flexible part, like the lyres of the LHC main busbars [7], or expansion loops. The IR busbars will have expansion loops similar in design to those currently installed in the LHC MQXB IR magnets [8].

### *2.3 18 kA Nb-Ti busbar insulation requirements*

The goal of the busbar insulation system is to prevent electrical contact between the busbars and the grounded cold mass, in order to withstand the voltage levels specified in [9].

The mechanical properties of materials are chosen to withstand stresses caused by Lorentz forces as well as thermal expansion mismatch of components [10], and have sufficient fracture toughness and ability of crack arrest to avoid crack propagation.

In order to avoid high mechanical stresses during cooling due to thermal expansion mismatch between busbar constituents and cold mass, it is advantageous to have the thermal expansion behavior of the bus insulation and housing be as similar to that of the busbar and stainless steel as possible.

As all materials of the busbar insulation system are inside the MQXF magnet cold masse they have to be non-magnetic and compatible with superfluid helium at 1.9 K. In addition they must provide sufficient radiation hardness in order to withstand the total absorbed dose over the entire HL- LHC lifetime. The peak integrated dose in the IT quadrupole magnet coil is 30 MGy [11]. The dose absorbed in the busbar insulation will be significantly lower.

The insulation material must be compatible with the chemicals that are used in the LHC for instance for screw locking or insulation purposes, in particular with Araldite 2011® two-component epoxy adhesive, Araldite 2012® fast curing, two-component epoxy adhesive, and ORAPI Freinage Moyen 303® (1,2,3,4-Tetrahydroquinoline) that is used for locking of stainless steel screws.

*2.3.1 Rigid busbar insulation and fixed point.* An insulating material commonly used for rigid applications in the cryogenic environment of the LHC is glass fibre reinforced epoxy EPGC 203 (EPGC 203 is equivalent to grade G11). This material was used to fabricate a busbar housing and the fixed point (six degrees of freedom) insulation (Figure 4). The main and return busbars, each consisting of two 18 kA Rutherford cables that are soldered together, are each insulated with polyimide film [12], held in place and electrically insulated from the grounded cold mass by glass fiber reinforced epoxy EPGC 203 housings. In order to provide a redundant insulation between the busbars an EPGC 203 spacer is added.

By rigidly mounting the busbar on one point of the coldmass it can be assured that the thermal longitudinal displacement of the busbar occurs solely on the busbar expansion loop. A cross section through a newly designed fixed point is shown in Figure 3 (a). The busbar cable is soldered to the copper profiles (Figure 3 (b)), which are maintained in glass fibre reinforced epoxy EPGC 203 (tradename ISOVAL®11) [13] housing. A 3D model and a photograph of the manufactured prototype busbar with fixed point are shown in Figure 4.

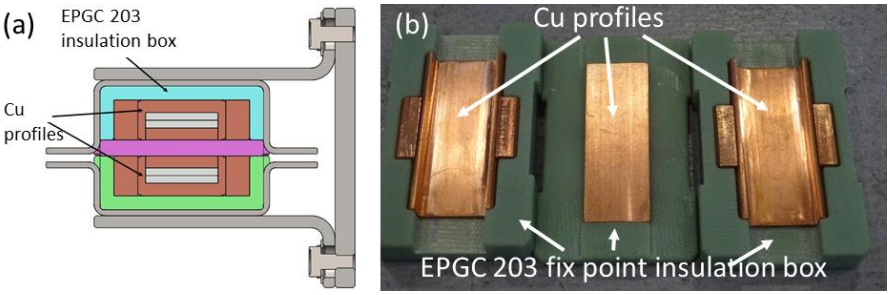


**Figure 3:** (a) Drawing of the fix point cross section. (b) Photograph of the fix components.

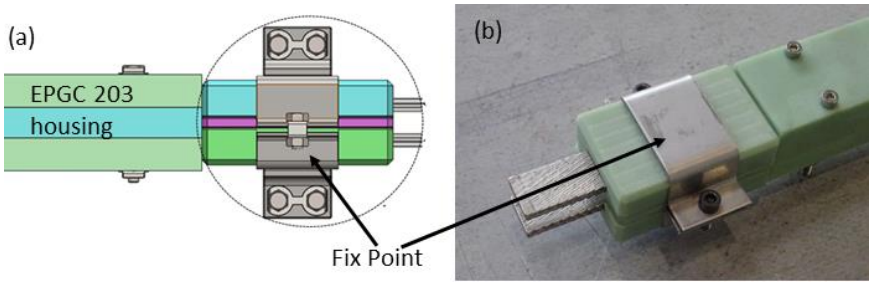


**Figure 4:** (a) 3D model of internal double 18 kA busbars with EPGC 203 housing and fixed point. (b) Photograph of busbar and fixed point prototype.

*2.3.2 Flexible busbar insulation.* Flexible expansion loops or lyres are needed to accommodate thermal expansion mismatch during cooling. The LHC main busbars and the 11 T dipole busbars have lyres [7] for this purpose, while the presently installed IR magnet busbars have expansion loops.

The LHC lyres are electrically insulated with two layers of polyimide tape wound in opposite direction with overlapping of 50 %. The external pre-impregnated layer is replaced by rings of polymerized fiberglass tape to hold the two polyimide layers. In addition each lyre is embedded in a glass–cloth sleeve [14] in order to provide further mechanical and electrical stability.

Alternative insulation solutions have been investigated, and in particular tubes made of PEEK are considered either as a replacement, or in addition to the glass fibre socket presently used in the LHC. This provides a redundant insulation system for flexible busbars. For the first time this solution is applied in the busbars of the 11 T dipole series magnets (Figure 5).

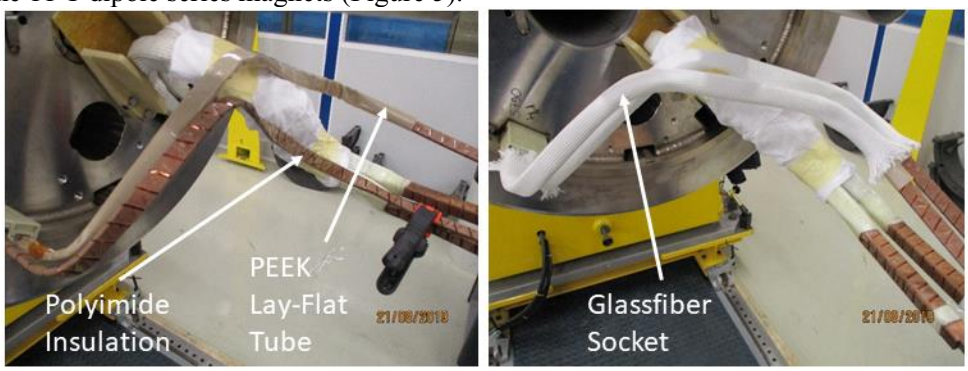


**Figure 5:** Flexible insulation on 11 T dipole busbar consisting of polyimide wrap, isopreg, PEEK lay flat® tube and glassfiber socket.

PEEK tubes are commercially available, also as corrugated tubes (Figure 6), which may be preferable for round cable insulation. The thin walled PEEK tubes resist sharp bends without failure. Materials compatibility with e.g. Araldite 2011® and 2012, which are commonly used in the LHC have been successfully verified.

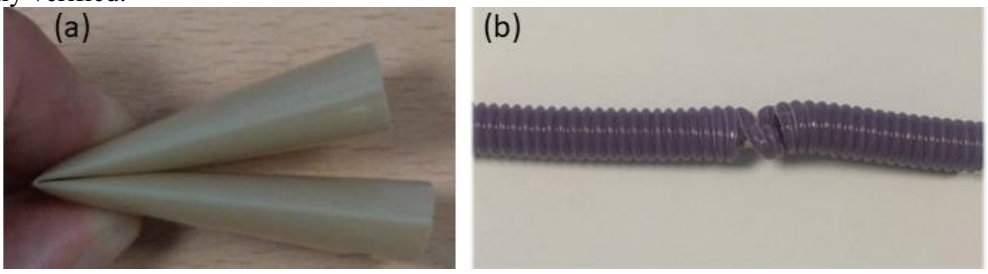


**Figure 6:** Flexible insulation on 11 T dipole busbar consisting of polyimide wrap, isopreg, PEEK lay flat® tube and glass fibre socket.

Radiation hardness of the HL-LHC busbar insulation is essential, and PEEK exhibits favourable radiation resistance as compared to other commonly used insulation materials [15].

## 3. Busbar splice production and testing

*3.1 MQXF Nb-Ti Rutherford lead cable splice*

Interconnecting Rutherford cables is conveniently done by soft soldering with either resistive or inductive heating, in a similar way as it is done for the LHC 13 kA busbar splices [16]. A commonly used solder is Sn96Ag4, which has good mechanical properties and very low electrical resistivity at cryogenic temperatures [17],[5].

*In situ* testing of Rutherford cable splice resistance in the LHC is performed at cold at high currents [18]. From ambient temperature tests it is not possible to predict the splice resistance at cold. Therefore, the splice

manufacturing and tooling validation are done using witness samples. Very high test currents of several thousand Amperes are needed to measure the very low resistances of superconductor Rutherford cable splices by the four-wire method. An alternative method is the measurement of the current decay constant in test loops with known inductance [19]. Such loops are routinely produced at CERN as Nb-Ti Rutherford cable splice witness samples, in order to validate the splice production processes and tooling.

The decay constant of the MQXF Nb-Ti lead cable loops with 120 mm splice overlap is $\tau$=888±102 s (average value obtained for three loops). Assuming a loop inductance of 300 nH [20], a MQXF lead cable splice resistance of 0.34 nΩ is derived.

### *3.2 MQXF Nb-Ti Rutherford lead cable to $Nb_3Sn$ coil splice*

Unlike for the ductile Nb-Ti cables, it is not possible to produce entire loops out of brittle $Nb_3Sn$ cables. In order to measure the resistance of the MQXF coil to lead cable splice, we have produced loops made of Nb-Ti lead cable, which was interconnected with a 120 mm long reacted MQXF $Nb_3Sn$ cable. In order to protect the brittle Nb3Sn cable from mechanical damage, Cu sheets are soldered on top and bottom of the splice. A schematic view of the splice produced to validate the MQXF coil to magnet lead splices is presented in Figure 7. During manufacturing of $Nb_3Sn$ cable splices special care needs to be taken not to exceed critical transverse mechanical pressures that could degrade the brittle $Nb_3Sn$ filaments [21].

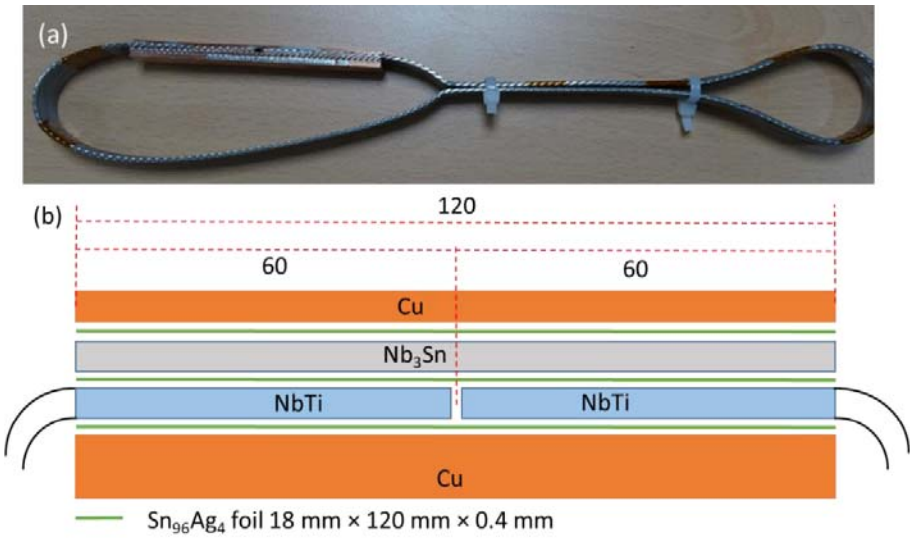


**Figure 7:** (a) Test loop for current decay constant measurements with two 60 mm-overlap MQXF Nb3Sn coil to Nb-Ti lead cable splices. (b) Schematic view of the Nb3Sn to Nb-Ti Rutherford cable splice assembly.

From the current decay constant of $\tau$=180 s measured for the loop with two 60 mm overlap splices in series, and the loop inductance of approximately 300 nH, a resistance value of 0.8 nΩ per 60 mm overlap splices is calculated.

Resistance measurements of flat Rutherford type cable splices with different intercable contact lengths at 4.3 K in self-field have confirmed that the splice resistance is inversely proportional to the splice overlap length, regardless if the splice overlap length exceeds the cable transposition pitch [20]. Since the overlap length of a MQXF $Nb_3Sn$/Nb-Ti splice is 120 mm, a resistance of 0.4 nΩ can be predicted for the MQXF coil to lead splices.

### *3.3 MQXF Nb-Ti Rutherford lead cable to round 18 kA trim cable splice*

Prototype splices were produced with two different round 18 kA cables. The splice design takes into account splice performance, ease of production, as well as the possibility for non-destructive testing of the solder connections.

The round cable is first soldered to the Cu housing using Sn96Ag4 solder with a melting temperature range between 221 °C - 225 °C. Afterwards the assembly is soldered onto the flat Rutherford cable busbar using Sn60Pb40 solder. The Sn60Pb40 solder is chosen for its lower melting temperature range between 183 °C – 188 °C, in order to prevent de-soldering of the previously soldered round cable (Figure 8).

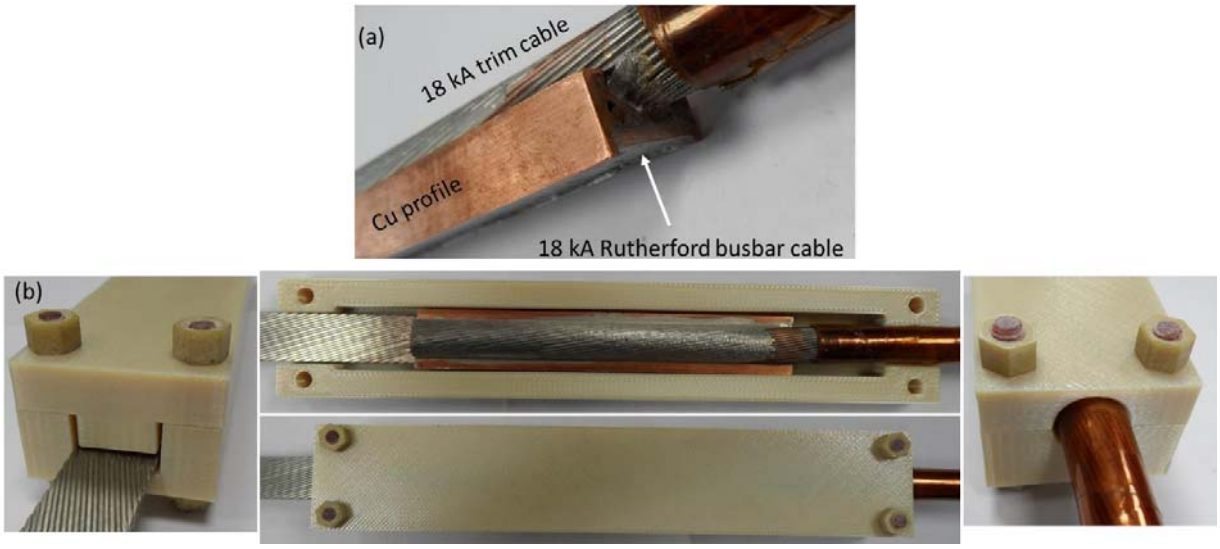


**Figure 8:** (a) Photograph of 18 kA trim cable to Rutherford cable internal busbar splice. (b) Prototype insulation box 3D printed from ULTEM9085 for the 18 kA splice.

In the final assembly the splice will be electrically insulated by an insulation box made of EP GC 203. For the tests a prototype insulation box produced from ULTEM9085 by fused deposition modelling, is used.

The round cable to Cu housing solder connection and the round cable stabilisation have been verified by micro-tomography [22]. The cable stabilisation and cable to Cu profile joint can be seen in great detail in the tomographic slices shown in Figure 9.

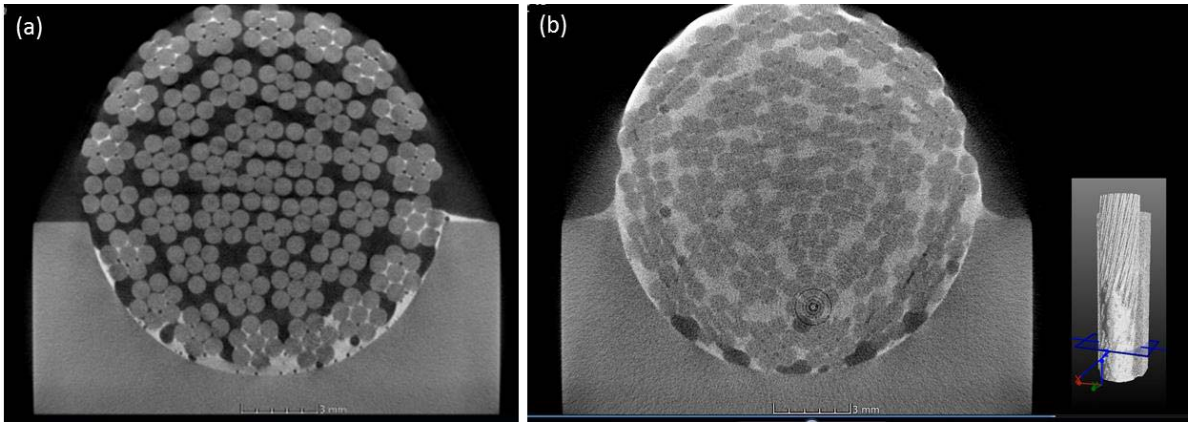


**Figure 9:** Micro-tomography cross section of 18 kA trim cable to splice Cu profile solder connection at (a) the extremity and (b) in 4 cm distance from the extremity (micro-tomography courtesy M. Jedrychowski).

The splice quality has also been verified by four-point resistance measurements using a digital micro-ohmmeter, with a test current of 10 A at ambient temperature [23]. The configuration of the measurement probes with two spring loaded pins each for current injection and voltage tap measurement are shown in Figure 10 (a). The resistance results presented in Figure 10 (b) are consistent with the micro-tomography observations. It can be seen that a low resistance of 2 μΩ is measured along 12 cm in the splice center that is well stabilised. At the splice ends the resistance increases due to lower solder filling of the cable that is revealed by the micro-tomography.

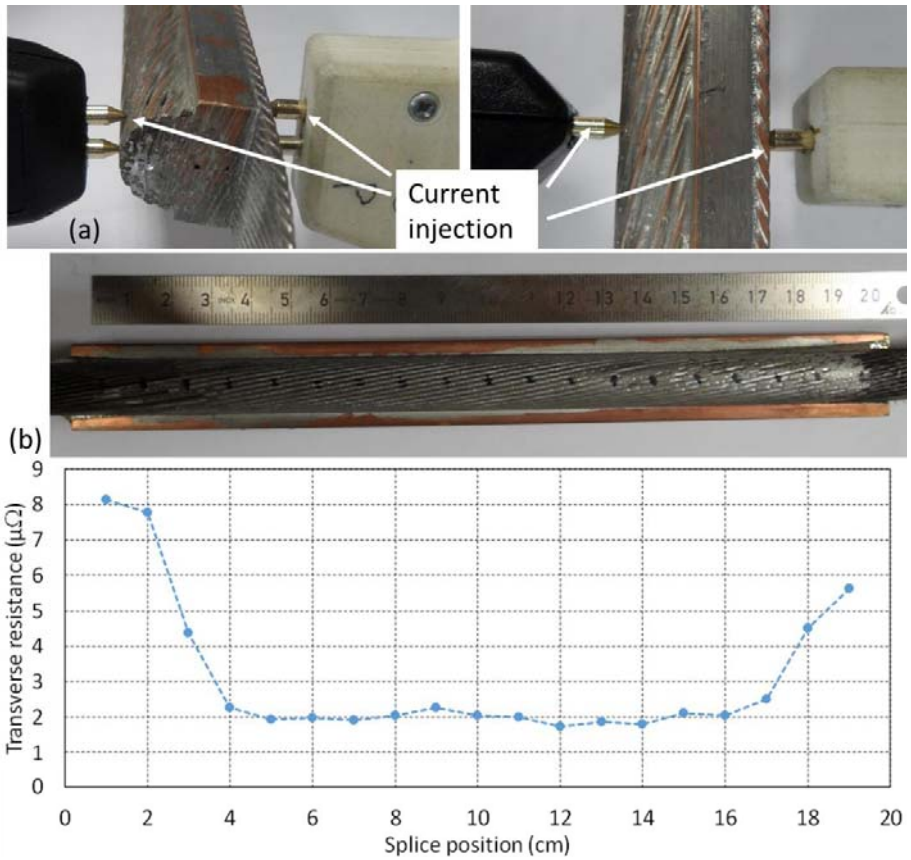


**Figure 10:** (a) Photograph of 18 kA trim cable to Rutherford cable internal busbar splice cross section with the spring loaded current injector pins and voltage tap (P) pins used for the electrical resistance maps with the micro-Ohm tester. (b) Cable with resistance measurement positions and corresponding resistance results.

## 4. Discussion and Conclusion

A concept for the fixation of the HL-LHC busbars in the MQXFB quadrupole coldmasses has been designed and prototype busbars with fixed point and insulation were produced.

The robustness of the electrical insulation of the busbars is crucial for the reliable operation of the HL-LHC magnets, which will be exposed to comparatively high radiation doses. An alternative insulation system for flexible busbar parts using thin PEEK tubes as a redundant insulation is proposed. The mechanical behaviour of different commercially available PEEK tubes has been tested. PEEK Lay-Flat tubes have been installed in addition to the polyimide films on the 11 T dipole busbars. Corrugated PEEK tubes are tested as an alternative busbar insulation, in particular for round cables.

18 kA round cable to Rutherford prototype cable splices were produced. The splice design enables non-destructive tests of the solder quality along the splice at ambient temperature. In a next step the splice performance will be measured at cryogenic temperature up to 18 kA.

## Acknowledgements

We would like to thank the members of the LMF busbar team for the production of busbar splices and test loops, and to M. Jedrychowski, CERN EN-MME for the micro-tomography of splices and busbars. We are also grateful to S. Feher, R. Bossert and M. Baldini from Fermilab for helpful discussions and advice.

## References

[1] The High Luminosity Large Hadron Collider, ed. O. Bruening and L. Rossi, World Scientific Publishing Co, (2015)

[2] L. Bottura, G. de Rijk, L. Rossi, E. Todesco, "Advanced accelerator magnets for upgrading the LHC," IEEE Trans. Appl. Supercond., 22(3), (2012). Art. No.4002008

[3] E. Todesco et al, Busbars for Q1 to D1 magnets", https://indico.cern.ch/event/830202/contributions/3476759/attachments/1867092/3070601/et_busbar_2019-06-21.pdf

[4] C. Scheuerlein, I. Pong, C. Senatore, M. Di Michiel, L. Thilly, A. Gerardin, B. Rehmer, L. Oberli, G. Willering, L. Bottura, "Temperature induced degradation of Nb-Ti/Cu composite superconductors", J. Phys.: Conf. Ser. 234 , (2010), 022031

[5] D. Schoerling, S. Heck, C. Scheuerlein, S. Atieh, R. Schaefer, "Electrical resistance of Nb3Sn/Cu splices produced by electromagnetic pulse technology and soft soldering", Supercond. Sci. Technol. 25 (2012) 025006

[6] M. Baldini et al, "Characterization of NbTi busbar for HL LHC Interaction Region Quadrupoles", submitted to IEEE Trans. Appl. Supercond.,

[7] R. Principe, P. Fessia, E. Fornasiere, (2011). 13 kA Superconducting Busbars Manufacturing Process", IEEE Trans. Appl. Supercond., 22(3), 4801604-4801604.

[8] R. Bossert et al, "Construction Experience with MQXB Quadrupole Magnets Built at Fermilab for the LHC Interaction Regions," IEEE Trans. Appl. Supercond. Vol. 12, No. 1, pp. 1297-1300, 2002.

[9] Engineering specification, "Voltage Withstand Levels for Electrical Insulation Tests on Components and Bus Bar Cross Sections for the Different LHC Machine Circuits", CERN, LHC-PM-ES-0001 rev. 2.0, EDMS No 90327, 2004

[10] C. Scheuerlein, B. Rehmer, M. Finn, C. Meyer, M. Amez-Droz, F. Meuter, K. Konstantopoulou, F. Lackner, F. Savary, J.-Ph. Tock, "Thermomechanical properties of polymers for use in superconducting magnets", IEEE Trans. Appl. Supercond., vol. 29, no. 5, 2019, Art. no. 7701605

[11] HL-LHC Preliminary Design Report, CERN-ACC-2014-0300, (2014)

[12] R. Bossert, "Status of bus and interconnect", at 8th HL-LHC collaboration meeting, (2018), https://indico.cern.ch/event/742082/contributions/3141508/attachments/1734744/2805370/Bus_and_Int_-_Hi-Lumi_oct_2018.pdf

[13] EN60893-3-2:2004, "Insulating materials - Industrial rigid laminated sheets based on thermosetting resins for electric purposes"

[14] L. Belova, M. Genet, J.-L. Perinet-Marquet, P. Ivanov, C. Urpin, "Design and Manufacture of the Superconducting Bus-Bars for the LHC Main Magnets", IEEE Trans. Appl. Supercond., vol. 12, (2002), 1305-1309

[15] T. Seguchi, Y. Morita, "Radiation resistance of plastics and elastomers", Polymer Handbook, 4, 583, (1999)

[16] A. Jacquemod, A. Poncet, F. Schauf, B. Skoczen, J.Ph. Tock, "Inductive Soldering of the Junctions of the Main Superconducting Bus Bars of the LHC", IEEE Trans. Appl. Superond. 18(2), 2008

[17] F. Heringhaus, T.A. Painter, "Magnetoresistance of selected Sn- and Pb-based solders at 4.2 K", Mater. Lett. 57 787, (2002)

[18] Z. Charifoulline, M.J. Bednarek, R. Denz, S. Le Naour, C. Scheuerlein, A. Siemko, J. Steckert, J.Ph. Tock, A. Verweij, M. Zerlauth, "Resistance of splices in the LHC Main Superconducting Magnet Circuits at 1.9 K", IEEE Trans. Appl. Superond. 28(3), DOI: 10.1109/TASC.2017.2784355

[19] R. Herzog and D. Hagedorn, "Inductive method to measure very small joint resistances of superconducting wires," in 17th International Cryo-genic Engineering Conference, Bournemouth, UK, 1988, pp. 495–498, IOP, Bristol, 1998.

[20] S. Heck, C. Scheuerlein, J. Fleiter, A. Ballarino, L. Bottura, "The electrical resistance of Rutherford type superconducting cable splices", IEEE Trans. Appl. Supercond., 25(3), (2015), 4800404

[21] P. Ebermann, J. Bernardi, J. Fleiter, F. Lackner, F. Meuter, M. Pieler, C. Scheuerlein, D. Schoerling, F. Wolf, A. Ballarino, L. Bottura, D. Tommasini, F. Savary, M. Eisterer, "Irreversible degradation of Nb3Sn Rutherford cables due to transversal compression stress at room temperature", Supercond. Sci. Technol. 31, (2018), 065009, (10 pp)

[22] M. Jedrychowski, "X-rays see all", CERN, (2018), https://home.cern/news/news/engineering/x-rays-see-all

[23] S. Heck et al, :" Non-destructive testing and quality control of the LHC main interconnection splices", IEEE Trans. Appl. Supercond., 25(2), (2014), 4000108